Dynamic Mechanical Study of Sodium Sulfonated Random Ionomers Based on Hydrogenated Styrene−Butadiene Copolymer

Mitsuo Nishida† and Adi Eisenberg*

Department of Chemistry, McGill University, 801 Sherbrooke Street West, Montreal, Quebec H3A 2K6, Canada

Received September 11, 1995; Revised Manuscript Received November 20, 1995⊗

ABSTRACT: Sodium sulfonated poly(styrene−ethylene−butylene) random ionomers [P(SEB-*co*-SSNa)] were obtained by hydrogenation, sulfonation, and neutralization of styrene−butadiene copolymers containing 45 wt % styrene. The dynamic mechanical properties were measured as a function of temperature for ionomers of a wide range of ion contents. Most of the ionomers showed two glass transitions, as well as a well-developed ionic plateau region in the storage modulus between the two glass transitions. The loss tangent peak of the upper T_g appeared below the decomposition temperature of the polymer, which permitted its detailed analysis as a function of ion concentration. The results of this study are explained on the basis of a recent model of morphology of ionomers in the solid state (the EHM model) and compared with those of the styrene−sodium methacrylate copolymers [P(S-*co*-MANa)] and sodium sulfonated polystyrene [P(S-*co*-SSNa)]. Considerable similarities exist in the properties of the matrix phase in the P(SEB-*co*-SSNa) and P(S-*co*-MANa) ionomer systems, in spite of the differences in composition. The P(SEB-*co*-SSNa) and P(S-*co*-SSNa) ionomer systems show similarities in the properties of the cluster phases, which, however, differ from those in the P(S-*co*-MANa). A detailed analysis of the storage modulus and the loss tangent curves showed that the storage modulus in the ionic plateau region is controlled by a filler effect of the dispersed phase (cluster or matrix) when there is only one continuous phase in the system. The storage modulus changes according to the logarithmic mixing rule when both the matrix and cluster phases are cocontinuous. Also, percolation theory can be applied to the modulus values of the P(SEB-*co*-SSNa) ionomer system.

1. Introduction

Random ionomers are usually composed of copolymers containing relatively few ions placed randomly along the chains. These polymers have many interesting properties which are attributable to both the nonionic host polymers and the ionic moieties and their interaction.[1] These properties can be changed or affected by such factors as the nature and the content of the ions, ion placement, presence and nature of plasticizers, etc. For example, most random ionomers in bulk show an ionic plateau or inflection region in the storage modulus between the glass transition and the flow region, which is due to ionic aggregation. The value of the modulus in that region can be varied over wide ranges by appropriate selection of the parameters mentioned above. Other properties that can be varied over wide ranges are the conductivity and permselectivity of ionomer membranes,[2] which again depend on amount and type of ionic groups, structure of the host polymer, etc. For these reasons, among others, a number of investigations of random ionomers have been performed in both academic and industrial laboratories. Representative ionomers are sulfonated polystyrene, styrene−methacrylic acid copolymers, ethylene−methacrylic acid copolymers, sulfonated ethylene−propylene−diene terpolymers (sulfonated EPDM), perfluorosulfonate or perfluorocarboxylate polymers, and the telechelics, among others. Ionomers have found applications in packagings, as elastomers, adhesives, polymer additives, and rheology modifiers, among others.

During the past three decades, many investigations have been devoted to random ionomers in the solid state. Small-angle X-ray scattering measurement (SAXS) showed that ionic aggregates, which are effective as scattering centers, exist in many random ionomers.[3−8] These aggregates or scattering centers have been termed multiplets.[9] Dynamic mechanical studies have revealed the existence of two glass transition temperatures (two T_gs) in many ionomers.[10−14] The lower T_g has been identified as the T_g of the matrix containing some dispersed ions, while the upper T_g has been ascribed to the T_g of the ion-rich regions. Recently, Eisenberg, Hird, and Moore interpreted the upper T_g as due to the overlapping regions of restricted mobility, where multiplets restrict the mobility of adjacent polymer chains;[14] in that model (the EHM model), these overlapping regions are termed clusters.

Styrene−sodium methacrylate copolymers, P(S-*co*-MANa), have been investigated in the past.[10,15] Recently, Kim et al.[16] reinvestigated in detail the dynamic mechanical properties of P(S-*co*-MANa) and interpreted the results in terms of the EHM model. At a very low ion content, the ion pairs form multiplets surrounded by polymer with restricted mobility.[14] At somewhat higher ion contents (below 5 mol %), as the relative volume of the regions of restricted mobility increases with increasing ion content, the regions of restricted mobility overlap and form clusters.[14] The two volume fractions of the matrix and cluster, as judged from the area under the loss tangent peaks ascribed to the glass transitions of the respective regions, become equal at ca. 5 mol % of ions, which is very close to the percolation threshold for the material of restricted mobility (5.4 mol %).[16] In the range of intermediate ion contents (6−12 mol %) in that ionomer system, there are two cocontinuous phases of matrix and cluster. At a high ion content (above 12 mol %), the cluster phase becomes the only continuous phase in the system. Also, the increase of the storage modulus in the ionic plateau region with

* To whom correspondence should be addressed.
† On leave from Polymer Technical Center, Toyobo Co. Ltd., 2-1-1 Katata, Ohtsu, Shiga 520-02, Japan.
⊗ Abstract published in *Advance ACS Abstracts,* January 15, 1996.

0024-9297/96/2229-1507$12.00/0

increasing ion content was explained in terms of both a filler effect and percolation behavior.[16]

While a number of studies of sulfonated polystyrene have been published, a detailed analysis of type performed by Kim et al.[16] has not been attempted for sulfonated polystyrene ionomers. One of the reasons is that, for samples of intermediate and high ion content, the upper glass transition occurs at a temperature very close to the decomposition temperature of polystyrene.[17,18] This high value of the cluster T_g of sulfonated polystyrene has been ascribed to the strong interaction between metal sulfonate ion pairs and the consequent slow ion hopping in the study by Hird and Eisenberg.[17] Therefore, in order to study the detailed relationship between the morphology and the mechanical properties of sulfonated ionomers as well as that between the matrix T_g and the cluster T_g, it is necessary to find a sulfonated ionomer system in which the upper glass transition occurs at much lower temperature than in sulfonated polystyrene. This naturally implies that the lower glass transition also has to occur at much lower temperature.

A low-T_g sulfonated ionomer has been prepared based on the sulfonated EPDM system.[19] However, it has been difficult to obtain this ionomer with a relatively high degree of sulfonation. An alternative system which meets these criteria is a sulfonated ionomer based on hydrogenated styrene−butadiene random copolymers. In the hydrogenated form, because the phenyl ring remains unhydrogenated, this copolymer consists of styrene, ethylene, and butylene chains. Thus, only the phenyl ring can be sulfonated. Control of the sulfonation procedure can yield polymers of a wide degree of sulfonation, which still retain the glass transitions at much lower temperature than that of sulfonated polystyrene. Other advantages of this system are that the styrene−butadiene random copolymer is commercially available and that the copolymer of high styrene content is amorphous after hydrogenation.

Molnár performed the first study of sulfonated hydrogenated styrene−butadiene random copolymers.[20] This study served as the starting point of the present investigation. In that study, differential scanning calorimetry and wide-angle X-ray scattering measurements revealed that the styrene−butadiene random copolymer containing 45 wt % styrene was amorphous after hydrogenation, although the copolymers containing 5 and 23 wt % styrene were semicrystalline after hydrogenation. Moreover, it was found that the lower T_g of the sulfonated ionomers remained at around 0 °C. For these reasons, hydrogenated styrene−butadiene random copolymers were selected for the present study, specifically the copolymer containing 45 wt % styrene because of the absence of crystallinity.

2. Experimental Section

2.1. Materials. The styrene−butadiene random copolymer PSB (styrene content 45 wt %, Scientific Polymer Products Inc.) was purified by dissolving in toluene (3% w/v) and precipitating into an excess of methanol. The average molecular weight was 200 kg/mol from viscometry in toluene at 25 °C[20] (Mark−Houwink coefficients: $K = 5.25 \times 10^{-2}$ mL/g and $a = 0.667$, obtained for a styrene−butadiene random copolymer containing 25 wt % styrene).[21] Infrared spectroscopy and proton magnetic resonance spectroscopy (^{1}H NMR) indicated that the proportions of vinyl/*cis*/*trans* in the butadiene units were 20/10/70 mol %.[20] Reagent grade solvents and chemicals were used throughout except for *p*-xylene, which was used as a solvent for hydrogenation (HPLC grade, Aldrich Chemical Co., Inc.) and chloroform, which served as a solvent for sulfonation (spectroscopy grade, BDH Inc.).

2.2. Hydrogenation. PSB (30 g) was dissolved in 600 mL of *p*-xylene. Dissolved gases were removed by three freeze−pump−thaw cycles. The solution was placed into a 2 L Parr pressure reactor (Parr Instrument Co.) with either 0.66 or 0.99 g of Wilkinson's catalyst, tris(triphenylphosphine) rhodium(I) chloride (Aldrich). After the reactor was closed and purged with H_2 gas, the hydrogenation was allowed to proceed at 50 °C and 2.4 MPa (350 psi) for 10−36 h. The hydrogenated material, styrene−ethylene−butylene random copolymer (PSEB), was diluted by the addition of a mixture of chloroform and xylene (1/1 v/v) to yield a 1% (w/v) solution and was then precipitated into an excess of hot methanol (50 °C). This was repeated three times to remove as much of the residual catalyst as possible. The polymer was dried in a vacuum oven at 80 °C for 5 days and kept in a desiccator until use.

2.3. Sulfonation. A modification of the method of Thaler[22] was used for the sulfonation of PSEB. The sulfonation was typically carried out according to the following procedure: 3 g of PSEB was placed along with 150 mL of chloroform in a 250 mL round-bottom flask and stirred at 50 °C for 24 h. An appropriate amount of sulfonating reagent (see below) was charged into the solution, and the reaction proceeded at 50 °C for 12 h. Methanol (20 mL) was added to terminate the reaction. The product was recovered by steam stripping (for ionomers of low ion contents) or precipitation into an excess of anhydrous diethyl ether (for ionomers of high ion contents). The purification process involved washing and decanting in anhydrous diethyl ether and was repeated three times. The product was stored in a "wet" form in a sealed container until use, in order to avoid degradation by the sulfonic acid.[20,23]

In the present study, a 100 mL sulfonating reagent solution consisted of 3.7 mL of 99% $ClSO_3H$ (Aldrich), 12.8 g of lauric acid (Eastman Organic Chemicals), and chloroform, which produces lauryl sulfate. The premixed solution was kept in a freezer until use. An appropriate amount of reagent was 0.40 mL/g of polymer and per mole percent sulfonation needed if the conversion is 100%.

The starting material and the products were characterized by ^{1}H NMR and Fourier-transform IR spectroscopy (FTIR). ^{1}H NMR spectra were recorded on a 200 MHz Varian XL 200 spectrometer. Chloroform-*d* (MSD Isotopes) was used as the solvent for PSB and PSEB, while dimethyl-d_6 sulfoxide (Cambridge Isotope Laboratories) was used as the solvent for the ionomers. FTIR spectra were recorded on an Analect Model AQS-20 spectrometer. Samples were cast as thin films on KBr windows.

2.4. Sample Preparation and Dynamic Mechanical Property Measurements. The bulk neutralization of the samples with sodium ions was carried out as described below. The "wet" sulfonated polymer was dissolved in a mixture of xylene and 1-butanol (3/1 v/v, for ionomers of low ion contents) or in a mixture of methanol and tetrahydrofuran (1/1 v/v, for ionomers of high ion contents) [0.5% (w/v)]. An appropriate amount of sodium hydroxide solution in methanol (ca. 0.2 M) was added slowly after the determination of the sulfonation level with a standardized NaOH solution in methanol to a phenolphthalein end point. Some of the polymer solutions turned cloudy before 100% neutralization. Under those circumstances, the addition of 1-butanol or methanol to these solutions usually improved the clarity. The solvent was eliminated using a "Rotavapor", and the sample was further dried in the vacuum oven for 2 days at 150−170 °C, depending on the ion content. Just before the dynamic mechanical thermal analysis (DMTA) measurements, samples were molded at 200−250 °C under low pressure for 0.5−1 h, and the dimensions (length, width, and height) of the samples were measured; these were used for calculation of dynamic mechanical properties and also for the calculation of densities of samples, which had been weighed on an analytical balance.

DMTA measurements were performed with a dynamic mechanical thermal analyzer (Polymer Laboratories Inc.) at a heating rate of 1 °C/min. The measurement conditions and the data treatment were the same as those in the study by Kim et al.[16]

Table 1. Ion Contents and Volume Fractions of Ionomers

sample notation	ion content (mequiv/cm^3)	volume fraction		
		matrix	cluster	multiplet
PSEB	0.00	1.00	0.00	0.000
P(SEB-0.5-SSNa)	0.11	0.98	0.00	0.004
P(SEB-1.8-SSNa)	0.38	0.91	0.09	0.015
P(SEB-2.4-SSNa)	0.50	0.80	0.20	0.019
P(SEB-4.0-SSNa)	0.82	0.77	0.23	0.032
P(SEB-5.4-SSNa)	1.09	0.59	0.41	0.042
P(SEB-5.8-SSNa)	1.17	0.57	0.43	0.045
P(SEB-7.2-SSNa)	1.42	0.54	0.46	0.055
P(SEB-7.6-SSNa)	1.50	0.45	0.55	0.058
P(SEB-7.7-SSNa)	1.52	0.43	0.57	0.059
P(SEB-9.0-SSNa)	1.75	0.22	0.78	0.068
P(SEB-12-SSNa)	2.27	0.11	0.89	0.089
P(SEB-15-SSNa)	2.79	0.09	0.91	0.108
P(SEB-18-SSNa)	3.28	0.05	0.95	0.127

3. Results

3.1. Synthesis. 3.1.1. Hydrogenation. During the hydrogenation of PSB, 1,2-butadiene (vinyl forms) and 1,4-butadiene (*trans* and *cis* form) changed into butylene and ethylene, respectively. The efficiency of the hydrogenation was monitored by FTIR spectroscopy. The FTIR spectra of PSB showed clearly the diene bands at 965, 995 (*trans* form), and 910 cm^{-1} (vinyl form), but the diene band due to the *cis* form at ca. 750 cm^{-1} was not seen clearly because of interference by the styrene band at 760 cm^{-1}. The diene band due to the vinyl form disappeared a few hours after the start of the reaction, while those from the *trans* form took ca. 25 h to disappear. Guo et al.[24] showed that the dienes act as the reaction sites in the rate-determining step for the selective hydrogenation of styrene−butadiene block copolymers. The reason for the difference in hydrogenation rates may be that the vinyl-form dienes are easier for the catalyst to approach than the *trans*-form dienes. This result is consistent with the results for polybutadiene.[25] On the other hand, the bands from styrene at 700 and 760 cm^{-1} did not change during hydrogenation. In addition, NMR spectra showed the complete elimination of the olefinic resonance in the 4−6 ppm region for the PSEB. These results suggest that the hydrogenation was essentially quantitative.

3.1.2. Sulfonation. Table 1 shows sulfonation levels for all the ionomers which were used in this study. The notation for the ionomer samples is P(SEB-*x*-SSNa); *x* is the mol % of sodium sulfonated styrene. Before sulfonation, the host copolymer, PSEB, is composed of 73 mol % of ethylene, 8 mol % of butylene, and 19 mol % of styrene. Because the content of styrene in the PSEB is only 19 mol %, the value of *x* does not exceed 19. The sulfonation levels obtained by titration agreed with those obtained from the analysis in the FTIR spectra of the bands at 1200 cm^{-1} (stretching vibration of SO_2 of the sodium sulfonated styrene unit)[26] and at 700 cm^{-1} (out-of-plane CH deformation on unsubstituted polystyrene). The NMR spectra of P(SEB-co-SSNa) showed a peak at 7.5 ppm due to the aromatic protons adjacent to the sulfonate group on the styrene unit. On the other hand, the spectra did not show any peaks at 4.0−5.0 ppm or at 6.6 ppm, which means that none of the sulfonate ions were attached to aliphatic carbons.[27]

When stoichiometric amounts of the sulfonating agents were used, the conversions were found to be between 40 and 90%. These results agree with those for the same sulfonation method used by Molnár[20] (40−50% conversion) and the sulfonation of styrene−butadiene diblock copolymers by Weiss et al. (50−60% conversion).[28]

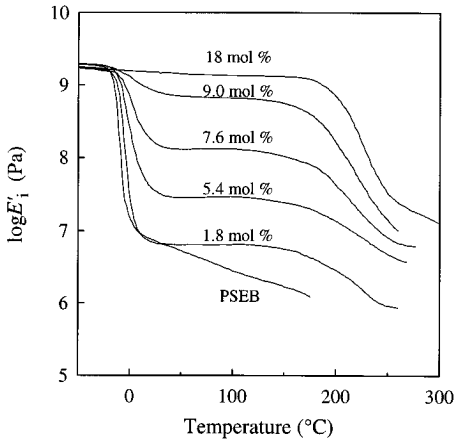

Figure 1. Plots as a function of temperature at 1 Hz of the logarithm of the storage modulus (E') for PSEB and P(SEB-*co*-SSNa) samples. The molar ion content is indicated for each sample.

3.2. Dynamic Mechanical Properties. All results were obtained in the same way as those for the styrene−sodium methacrylate copolymers studied by Kim et al.[16] Figures A(a)−(c) in the supporting information show representative data for the P(SEB-7.6-SSNa). For example, this ionomer is glassy below −20 °C, goes through the glass transition of the matrix phase between −20 and +20 °C, and exhibits an ionic plateau region between 20 and 180 °C. The glass transition of the cluster phase occurs between 180 and 250 °C, a short rubbery region is seen between 250 and 310 °C, and finally the flow region is seen above 310 °C.

A number of numerical values are obtained from the plots of log E', log E'', and loss tangent vs temperature. From the first of these, in the plot of log E' at 1 Hz, m_m and m_c indicate, respectively, the slopes of the plot in the region of the glass transition of the matrix and the cluster; in addition, E'_g, and E'_i indicate, respectively, the storage modulus in the glassy region (at −40 °C) and at the ionic plateau (at 50 °C). From the plot of log E'' at 1 Hz, $T''_{g,m}$ and $T''_{g,c}$ are obtained from the positions of the peak maxima of the glass transitions of the matrix and cluster regions, respectively. In the plot of the loss tangent (tan δ) at 1 Hz, A_m and A_c are, respectively, the peak areas of the glass transitions of the matrix and cluster regions. Also the peak maxima ($T_{g,m}$ and $T_{g,c}$), the peak heights (H_m and H_c), and the peak widths at half-height (W_m and W_c) of the two glass transitions are obtained from the plot. It should be mentioned that these ionomers show a third tan δ peak in addition to the peaks of the glass transitions of the matrix and cluster regions. This peak appears at 240−300 °C in each ionomer. The presence of a high-temperature peak above T_g was also seen in other polymer systems, including ionomers. In some cases, it was called "dynamic cross-linking" and ascribed to the decomposition and cross-linking of the polymer, in studies by Lee and Goldfarb[29] and by Gauthier and Eisenberg.[30] The peak area was ca. 10% of the sum of the values of A_m and A_c. The peak position and area were found to be independent of ion concentration. The values of A_c were obtained after the elimination of the value of the third peak from the overlapping peaks.

Figure 1 shows a plot of log E' of some P(SEB-*co*-SSNa) ionomers as a function of temperature; for the sake of clarity, not all curves are shown. The nonionic PSEB shows the glassy, the glass transition, and the rubbery regions. The shape of the log E' curve in the rubbery region is very similar to that of amorphous

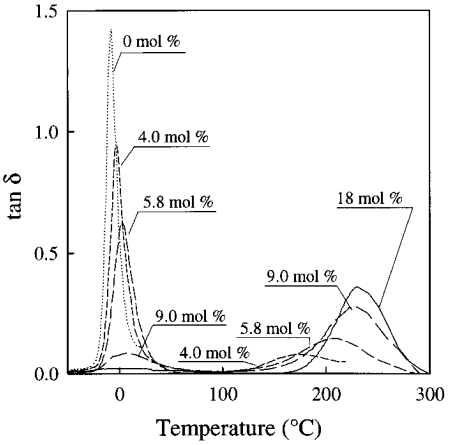

Figure 2. Plots as a function of temperature at 1 Hz of the loss tangent (tan δ) for PSEB and P(SEB-co-SSNa) samples. The molar ion content is indicated for each sample.

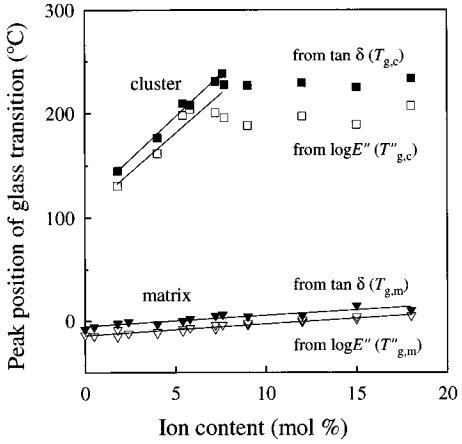

Figure 3. Lower plots, peak positions for the glass transition of the matrix from tan δ (▼) and log E'' (▽) versus ion content (mol %); upper plots, peak positions of the glass transition of the cluster phase from tan δ (■) and log E'' (□) versus ion content (mol %). The straight lines are linear regression plots.

EPDM[31] and is quite different from that of amorphous polystyrene. Also, the ionomers containing more than 1.8 mol % sodium sulfonated styrene show a clear plateau region following the glass transition of the matrix, which is similar to that of zinc sulfonated EPDM.[31]

Figure 2 shows the tan δ curves of some ionomers after subtraction of the background and the decomposition peak; again, for the sake of clarity, not all curves are shown. It is seen that as the ion content increases, the peak of the glass transition of the matrix region decreases and that of the cluster region increases. Both move to higher temperatures. Each region will now be discussed in order of increasing temperature.

3.2.1. Glassy Region. DMTA measurements in the glassy region between −50 and −20 °C showed that the value of storage modulus for all the ionomers and the PSEB decreased by less than 0.05 log units. In addition, with increasing ion contents, the storage moduli E'_g were constant (log E'_g at −40 °C = 9.27 ± 0.05) within experimental error for all the ionomers and the PSEB, as shown in Table A in the supporting information. The constancy of the glassy modulus parallels that observed in the P(S-*co*-MANa) system,[16] for the identical reasons.

3.2.2. Glass Transition of the Matrix Phase. For all the ionomers and the PSEB, the storage moduli begin to decrease at ca. −20 °C due to the glass transition of the matrix phase, as shown in Figure 1. Peaks appear in the curves of log E'' (not shown here) and tan δ (Figure 2). The matrix T_gs ($T_{g,m}$s and $T''_{g,m}$s) from the peak maxima are plotted as a function of ion content in Figure 3. It is seen that the $T_{g,m}$ and $T''_{g,m}$ increase with increasing ion content, as is also seen in many other ionomer systems.[1b,16,17] The equations for the first-order fit are

$$T_{g,m}\,(°C) = -5 + 1.1x \quad (\text{from tan } \delta) \qquad (r^2 = 0.925)$$

$$T''_{g,m}\,(°C) = -14 + 1.1x \quad (\text{from log } E'') \qquad (r^2 = 0.965)$$

where x and r^2 are ion content (mol %) of the ionomers and the linear least-squares correlation coefficient, respectively.

The tan δ peak areas A_m and A_c are plotted as a function of ion content in Figure 4. A_m decreases and A_c increases with increasing ion content, in parallel with the behavior of P(S-*co*-MANa).[10,16] The data for A_m and A_c are linear in the range of 0−9 mol %, and a linear regression can be calculated. For A_m, the equation is

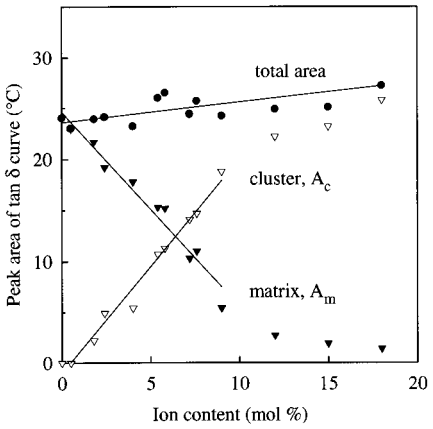

Figure 4. Peak areas of the tan δ curves for the glass transitions of the matrix (▼) and the cluster (▽), and the total peak areas (●) versus ion content (mol %).

$$A_m\,(°C) = 24.6 - 1.90x \qquad (r^2 = 0.982)$$

3.2.3. Ionic Plateau Region. The ionomers containing 1.8 mol % or more of ions exhibit an ionic plateau region as shown in Figure 1. Figure 5a shows the storage modulus E'_i in the ionic plateau region as a function of ion content. E'_i increases with increasing ion content until 9 mol %, above which it does not change appreciably. A detailed discussion of this trend is given in connection with the applicability of the filler concept. Figure 5b will be discussed later.

3.2.4. Glass Transition of the Cluster Phase. As shown in Figure 1, the storage modulus shows a major drop near 200 °C due to the glass transition of the clusters. Peaks appear in the curves of log E'' and tan δ (Figure 2), in agreement with the behavior of other ionomers.[10,16] The cluster T_gs ($T_{g,c}$s and $T''_{g,c}$s) from the peak maxima are plotted as a function of ion content in Figure 3. The $T_{g,c}$ and $T''_{g,c}$ increase with increasing ion content but do not change beyond an ion content of 8 mol %. The equations for the region below 8 mol % are

$$T_{g,c} = 115 + 16.3x \quad (\text{from tan } \delta) \qquad (r^2 = 0.993)$$

$$T''_{g,c} = 108 + 14.8x \quad (\text{from log } E'') \qquad (r^2 = 0.944)$$

A_c is plotted as a function of ion content along with the plots of A_m in Figure 4. A_c increases with increasing

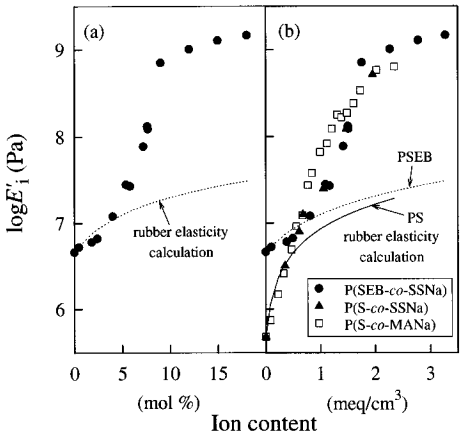

Figure 5. Plots of the log E' at the ionic plateau region (at 50 °C) versus ion content (a) (in mol %) for P(SEB-*co*-SSNa) (●) and (b) (in mequiv/cm^3) for the P(S-*co*-SSNa) (▲),[17] P(S-*co*-MANa) (□),[16] and P(SEB-*co*-SSNa) (●) (present study). The solid line and dotted lines represent the calculated values for the storage moduli of the matrix for the P(S-*co*-MANa)[16] and P(SEB-*co*-SSNa), respectively.

ion content. As before, if the values of A_c are considered for samples only below 10 mol %, the equation is

$$A_c = -1.0 + 2.10x \qquad (r^2 = 0.991)$$

In an earlier section, it was shown that A_m decreases with increasing ion content. A combined equation for A_m and A_c can be developed, which is $A_m + A_c = 23.6 + 0.20x$. Also a regression for all the data of the total area can be calculated, which is

$$A_m + A_c = 23.8 + 0.15x$$

Since the coefficient for x is small (0.15), it is seen that the total area is, for all practical purposes, independent of ion content, as was also seen in P(S-*co*-MANa).[10,16] Therefore, it is possible to take the ratios of A_m or A_c against the total area ($A_m + A_c$) as representative of the volume fractions of the matrix and cluster phases, respectively, as was done before.[10,16] Table 1 shows the results. This table also shows the volume fraction of multiplets, which can be calculated from the volume per atom of ion pairs and the density of ionomers in the same way as was done for P(S-*co*-MANa).[16] The volume per atom of sodium sulfonate ion pairs was calculated to be 1.29×10^{-2} nm^3/atom, which is an average of sodium sulfite and sodium sulfate.[32] The density of the ionomers was $0.95 + 0.011x$ (g/cm^3), where x is the ion content (mol %). All the data of the densities are shown in Table A of the supporting information. These volume fractions are discussed more extensively in a later section.

4. Discussion

As an introduction to the detailed discussion of the present ionomer system, it is useful to look at Figure 6, which shows the log E' at ca. 5.5 mol % ion content as a function of temperature at 1 Hz for three ionomer systems, P(SEB-5.4-SSNa), P(S-6.2-SSNa),[17] and P(S-4.9-MANa).[16] The P(SEB-5.4-SSNa) ionomer shows a well-developed ionic plateau region in the storage modulus, which results from the strong ionic interactions. In addition, because the matrix T_g is very low (relative to the styrene copolymers in the absence of ethylene−butylene) and because it increases only very slightly with ion content, the width of the ionic plateau is very much larger than that in the other ionomers.

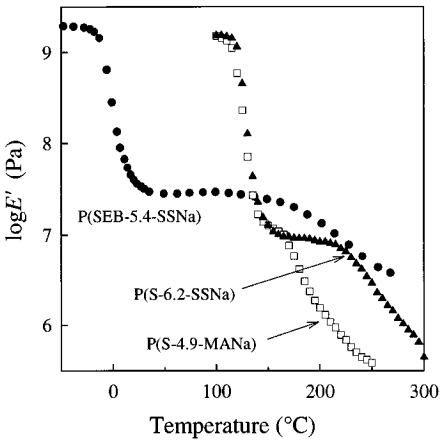

Figure 6. Plots of the log E' as a function of temperature at 1 Hz for P(SEB-5.4-SSNa) (●), P(S-4.9-SSNa) (▲),[17] and P(S-6.2-MANa) (□).[16]

Table 2. dT_g/dc [°C/mol % or °C/(mequiv/cm^3)] for Matrix and Cluster Phases in Three Ionomer Systems (from tan δ)

	dT_g/dc of matrix phase		dT_g/dc of cluster phase	
ionomer	°C/ mol %	°C/ (mequiv/cm^3)	°C/ mol %	°C/ (mequiv/cm^3)
P(SEB-*co*-SSNa)	1.1	6.4	16	80
P(S-*co*-SSNa)	3	30	6	70
P(S-*co*-MANa)	3	330	6	70

Furthermore, the width of the plateau increases with increasing ion content, in contrast to that in the other ionomers, e.g., P(S-*co*-SSNa) and P(S-*co*-MANa), where the widths of the plateau-like regions remain essentially constant.[16,17] The width of the ionic plateau in the present system is similar to that in sulfonated EPDM ionomer.[31] However, in contrast to the earlier system, in P(SEB-*co*-SSNa) the wide range of sulfonation levels yields a wide range of the storage moduli in the ionic plateau region. Thus, the P(SEB-*co*-SSNa) ionomer system might have some useful properties as an elastomer. In the present section, we discuss the properties and morphology of P(SEB-*co*-SSNa) and compare them with those of other ionomer systems, mainly P(S-*co*-SSNa) and P(S-*co*-MANa).

4.1. Matrix T_g and Cluster T_g. In the present system, both the matrix and cluster T_gs are observed clearly by DMTA measurements, and both increase with increasing ion content (see Figure 3), as they do in other ionomers. However, the rates of increase are different from those in the other systems based on polystyrene. For example, many of those ionomers show the slope for the matrix T_g versus ion content plot (dT_g/dc) to be in the range of 3−5 °C/mol % and for the cluster T_g to be in the range of 3−9 °C/mol %.[1b,10,16,17,30,33] The recent detailed analysis for P(S-*co*-SSNa)[17] and P(S-*co*-MANa)[16] ionomers shows the slopes for the cluster T_g to be in the range of 5−7 °C/mol %. In the present system, the values of dT_g/dc for the matrix and cluster T_g are found to be in the range of 1−2 and 14−17 °C/mol %, respectively.

When one compares an ionomer system with another ionomer system based on a different host polymer, it is necessary to consider differences in the size and mass of the repeat units. Therefore, in this section, ion concentration is expressed in equivalents per unit volume instead of mol %. Table 2 shows the result. For the matrix T_g, when ion content is expressed as mequiv/cm^3, the dT_g/dc for P(SEB-*co*-SSNa) changes from 1.1

Table 3. Discontinuity Ranges in Trends of Properties of Matrix and Cluster Phases versus Ion Contents [mol % and (mequiv/cm³)]

	matrix phase		cluster phase			
unit	log m_m	W_m	H_m and A_m	m_c	W_c	H_c and A_c
			P(SEB-*co*-SSNa)			
mol %	2−3	2−3 and 8−9	9	5 and 8−9	constant	8−9
mequiv/cm³	0.4−0.6	0.4−0.6 and 1.5−1.7	1.7	1.0 and 1.5−1.7	constant	1.5−1.7
			P(S-*co*-MANa)			
mol %	4−5	14	14 (log H_m)	12	4	4 (log H_c)
mequiv/cm³	0.4−0.5	1.5	1.5	1.3	0.4	0.4

°C/ mol % to 6.4 °C/(mequiv/cm³), while those for the P(S-*co*-SSNa) and P(S-*co*-MANa) systems based on polystyrene change from ca. 3 °C/mol % to ca. 30 °C/(mequiv/cm³). For other ionomer systems, the dT_g/dc for the ethylene−sodium acrylate copolymers, for example, is ca. 7 °C/(mequiv/cm³) (from log E'')[34] and that for the sulfonated polysulfone is ca. 50 °C/(mequiv/cm³) (from tan δ).[35] The ethylene−sodium acrylate copolymers show almost the same slope as that of P(SEB-*co*-SSNa), but the ionomers based on polystyrene do not. The polystyrene backbone is more rigid than that of styrene−ethylene−butylene copolymer or that of polyethylene. The reason for the difference of the slopes may be that an ionic cross-link in the ionomers based on polystyrene can affect a much larger volume than in P(SEB-*co*-SSNa) or in the ethylene−sodium acrylate copolymers. In addition, it should be recalled that the ionic groups are attached only to the phenyl rings, and that, therefore, multiplet formation represents to some extent an enhancement of the multiplet region by styrene and a corresponding depletion of styrene in the matrix.

For the cluster T_g, when the ion content is expressed as mequiv/cm³, the slope for P(SEB-*co*-SSNa) is ca. 80 °C/(mequiv/cm³), while those for P(S-*co*-SSNa) and P(S-*co*-MANa) are ca. 70 °C/(mequiv/cm³). There is, thus, no significant difference among the values of dT_g/dc for the cluster T_g for these ionomer systems. However, P(SEB-*co*-SSNa) shows a leveling off in the increase of the cluster T_g above ca. 8 mol % ion content, while the cluster T_gs of P(S-*co*-SSNa) and P(S-*co*-MANa) continue increasing with ion content in the ranges of 0−11 and 0−22 mol %, respectively. It should be mentioned that we cannot measure the cluster T_g in P(S-*co*-SSNa) above 16 mol % [=1.5 mequiv/cm³, equivalent to P(SEB-7.6-SSNa)] because the cluster T_g of P(S-*co*-SSNa) would be above the decomposition temperature of the polymer.[17,18] The cluster glass transition behavior, notably the leveling effect above 8 mol % of ions, is noteworthy. In the study of the P(S-*co*-MANa) system, it was found that at 22 mol % of ions, the cluster T_g was ca. 320 °C.[16] This value should be compared to the T_g of pure poly(sodium methacrylate), which has been estimated to be 350 °C. Thus, it is clear that in the range between 22 mol % of ions and 100 mol %, the T_g increases by less than ca. 30 °C. This is a profound leveling effect and underscores the degree of immobilization of the region in the immediate surroundings of the multiplet. The same effect is observable in the present system also.

4.2. Two Morphological Changes in the Matrix and Cluster Phases. In this section, the properties of the matrix and cluster phases other than the glass transitions are discussed. These other properties are the slopes of storage moduli (m_m and m_c), the widths at half-height of the tan δ peaks (W_m and W_c), the peak heights (H_m and H_c), and activation energies ($E_{a,m}$ and $E_{a,c}$). The supporting information shows all the data in Figures B and C. Table 3 shows the discontinuities in the trends of the properties of the matrix and cluster phases of P(SEB-*co*-SSNa) and P(S-*co*-MANa).[16] Of importance is that similarities exist in the ion contents at the discontinuities in properties between the matrix and cluster. It is found that two discontinuity ranges exist in the trends of the properties when plotted against ion content in the P(SEB-*co*-SSNa) system, in analogy with those found in the P(S-*co*-MANa) copolymers. One is found at low ion contents, i.e., 2−3 mol %, while the other is seen at higher ion contents, i.e., 8−9 mol %. The EHM model can interpret these two discontinuity ranges, as described below.

In the range of low ion contents (below 2 mol %), the matrix phase is homogeneous, although the cluster phase starts to form even at an ion content below 1.8 mol %. In that range, log(m_m) and W_m do not change with ion content. At a somewhat higher ion content (2−3 mol %), the cluster phase becomes cocontinuous, as will be shown in the discussion of filler and percolation effects. In the range of intermediate ion contents (3−8 mol %), the cluster phase expands; in parallel, however, the matrix phase becomes more heterogeneous. In that range, log(m_m) decreases and W_m increases with ion content. At high ion contents (8−9 mol %), the cluster phase probably becomes the only continuous phase. Here, the m_c increases substantially. At still higher ion contents (above 9 mol %), the matrix phase is no longer continuous. The cluster phase at this point can be called homogeneous, but it should be recalled that multiplets still retain their identity within this cluster phase. Thus, the cluster phase cannot be as uniform in composition as the matrix phase at low ion contents, which is probably reflected in the differences between the values of H_m and W_m at low ion contents, and those of H_c and W_c at high ion contents.

Table 3 expresses ion contents in two sets of units; mol % and mequiv/cm³. If one compares the properties of P(SEB-*co*-SSNa) with those of P(S-*co*-MANa) using the units of mequiv/cm³, it is seen that considerable similarities exist in the discontinuities in the trends of the matrix properties of P(SEB-*co*-SSNa) and P(S-*co*-MANa), in spite of the differences in composition. This is seen in the left part of the table. The result is not surprising if one thinks that the matrix phase is composed of nonionic material with some dispersed ions which can form only isolated ion pairs or multiplets. On the other hand, few similarities are seen in the discontinuities in the trends of the cluster properties of P(SEB-*co*-SSNa) and P(S-*co*-MANa), as can be seen in the right part of the table.

4.3. Phase Separation Behavior in View of Filler and Percolation Concepts. In the previous section, the two T_gs for matrix and cluster phases and two regions of morphological changes were discussed. It is clear that the present system shows a phase-separated behavior, which is seen in some systems of polyblends and block copolymers. This phase separation behavior can be analyzed in the light of filler and percolation concepts. In this section, the mechanical properties as expressed by the storage modulus E'_i in

the ionic plateau region and the morphology of P(SEB-*co*-SSNa) ionomers are discussed as a function of the volume fractions of the matrix phase, and of the cluster phase, and of multiplets, as well as the mole fraction of ions.

4.3.1. Regular and Inverted Filler Systems. At low ion contents, the cluster is the dispersed phase, while at high ion contents, the cluster becomes the only continuous phase. Thus, a phase inversion must occur at intermediate ion contents in the present system. Therefore, depending on the ion content, the materials should be regarded both as a regular system of rigid fillers in a soft continuous phase and as an inverted system of soft fillers in a rigid continuous phase.[36] To apply filler concepts to the present ionomer system, the Halpin−Tsai equation[37] is available, which has been applied to another ionomer system.[16] In addition, the equation can be applied not only to regular systems but also to inverted systems. However, it is necessary to keep in mind that in both the regular and inverted systems, the filler particles and the matrix should each have a constant modulus for all compositions. For the P(SEB-*co*-SSNa) ionomer system, the modulus values for the matrix phase can be assumed to be almost constant for the all ionomers, and those for the cluster phase can be assumed not to change at high ion contents above 8 mol %. These assumptions are reasonable in view of the relatively high modulus value of the rubbery PSEB and the constancy of the cluster T_g with increasing ion content beyond 8 mol %.

The Halpin−Tsai equations used for the interpretation of the regular and inverted systems as well as the modification for the present system are discussed in the supporting information. The modified equation for the regular system is

$$\frac{E'_i}{E'_m} = \frac{1 + A_{reg}B_{reg}\phi_c}{1 - B_{reg}\psi\phi_c}$$

where E'_i and E'_m are the storage moduli at the ionic plateau of the ionomer and at the rubbery plateau of the rubbery PSEB, respectively. A is a constant dependent on the geometry of the dispersed phase and Poisson's ratio of the continuous phase. B is a constant dependent on the relative moduli of the dispersed and continuous phases, ϕ_c is the volume fraction of the cluster phase, and ψ is a factor dependent on the maximum packing fraction of the dispersed phase in the regular system.

In the inverted system, the modification of the Halpin−Tsai equation is

$$\frac{E'_i}{E'_c} = \frac{1 - B_{inv}\psi\phi_m}{1 + A_{inv}B_{inv}\phi_m}$$

where E'_c is the glassy modulus of the ionomer, and ϕ_c is the volume fraction of the matrix phase.

Figure 7 shows a plot of the experimental values of E'_i and those calculated for the regular system and the inverted system against the volume fraction of the clusters. In the regular system, the calculated values coincide with the experimental values when the volume fraction of the cluster ϕ_c is below 0.2 ($\phi_m = 0.8$), and therefore the cluster phase is thought to act as a filler in that range. In the inverted system, the calculated values coincide with the experimental values when the volume fraction of the cluster ϕ_c is above 0.9, and therefore the matrix phase (the PSEB) is thought to act as filler particles in that range. Both phases are thought to be cocontinuous when the ϕ_c is between 0.2 and 0.9. Consequently, the maximum packing fraction of the cluster $\phi_{c,max}$ is 0.9, and the maximum packing fraction of the matrix $\phi_{m,max}$ is 0.8. When two systems are treated according to the logarithmic mixing rule, which holds in many polyblend systems,[36] the volume fraction of the rigid dispersed phase in the regular system ϕ_{reg} and the volume fraction of the soft dispersed phase in the inverted system ϕ_{inv} are calculated from the volume fractions for the matrix and cluster as shown below. The equations are

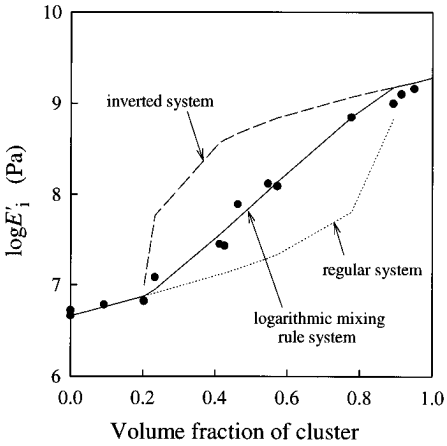

Figure 7. Plots of the log E' (●) at the ionic plateau versus the volume fraction of the cluster. The long-dashed line, dotted line, and solid line represent the calculated values for the inverted filler system, the regular filler system, and the logarithmic mixing rule system, respectively.

$$\log E'_i = \phi_{reg} \log E'_{reg} + \phi_{inv} \log E'_{inv}$$

$$\phi_{reg} = \frac{\phi_{c,max} - \phi_c}{\phi_{c,max} - (1 - \phi_{m,max})}$$

$$\phi_{inv} = \frac{\phi_{m,max} - \phi_m}{\phi_{m,max} - (1 - \phi_{c,max})}$$

E'_{reg} and E'_{inv} are, respectively, the storage moduli of the regular system and the inverted system. The calculated values agree with the experimental values over all volume fractions of the cluster phase as shown in Figure 7. The least-squares correlation coefficient is 0.986 for the combined results using all three equations.

Thus, one can conclude that the cluster phase acts as a filler at low volume fraction of the cluster ($\phi_c < 0.2$). In that range, the Halpin−Tsai equation for the regular system is employed. The cluster and matrix phases act as cocontinuous phases at intermediate volume fractions ($0.2 < \phi_c < 0.9$); in that range, the logarithmic mixing rule is applied. Finally, the matrix phase acts as the filler at high volume fraction of clusters ($\phi_c > 0.9$), and the Halpin−Tsai equation for inverted system is useful.

4.3.2. Percolation Behavior. As was pointed out in the previous section, the cluster phase changes from dispersed to cocontinuous phase in the range of 2−3 mol % of ions. In the same range, the storage modulus E'_i in the ionic plateau region increases steeply. It seems reasonable to suggest that the cluster phase goes through a percolation threshold when it begins to form a cocontinuous phase. Thus, it is of interest to explore percolation behavior in the present system, which is the object of this section. As was done in the discussion of filler systems, it is necessary to keep in mind that,

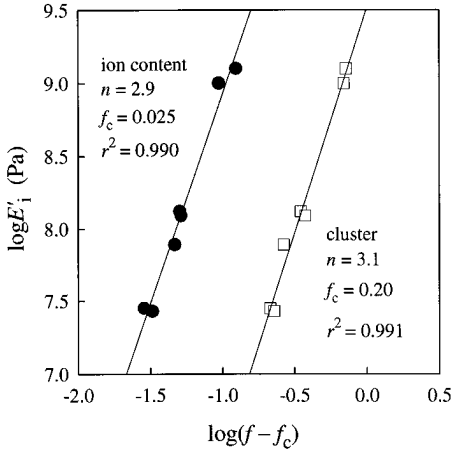

Figure 8. Plots of the the log E' at the ionic plateau versus the logarithm of $(f - f_c)$ (f = the fraction of percolating species, f_c = the critical fraction at the percolation threshold). n and r^2 represent the slope of the line (the critical exponent) and the linear-squares correlation coefficient, respectively.

according to the basic concept of percolation, the percolating species and the matrix should each have a constant modulus. This should be true at least near the percolation threshold if one wishes to compare percolation parameters in the present system with those in other systems. In the discussion of percolation behavior in the present system, the same assumptions, i.e., constancy of the moduli of the matrix and cluster for all compositions, are made, as in the section dealing with a filler system.

As before, the most realistic possibility in regard to the nature of the percolating species is the cluster phase. Figure 8 shows the logarithm of the storage modulus E'_i plotted against the logarithm of $(f - f_c)$, where f is the volume fraction of the clusters (or the mole fraction of the ions) and f_c is the critical volume fraction (or mole fraction) at the percolation threshold. The values f_c were chosen so as to obtain the best values of the least-squares correlation coefficient r^2 between log E'_i and log$(f - f_c)$. If percolation is operative in the present system, a plot of log E'_i against log$(f - f_c)$ should give a straight line with a slope n, where n is the critical exponent. A linear relation is, indeed, observed. While a percolation plot is also given for the ion content, it is not meant to imply that "ion content" is a percolating species. The plot is given only to illustrate the determination of the percolation threshold expressed as mol % ions.

First, the critical volume fraction is discussed. In this study, f_c for the clusters was found to be 0.20, and f_c for ion contents to be 0.025. The value for the cluster agrees with the theoretical value (0.198) for the site percolation threshold in a face-centered cubic lattice.[38] In addition, it is clear that this value of f_c for the clusters also agrees with the mole fraction of the ions (0.02−0.03) at which a discontinuity in the concentration profiles of several properties suggests the onset of a continuous cluster phase. It should be recalled that at a volume fraction of the clusters (ca. 0.2), the system no longer behaves as a regular filled system but begins to show transition to the inverted system (see Figure 7). This result reinforces the conclusions of the earlier sections that a morphological change in the matrix and cluster phases occurs at ion contents of 2−3 mol % and that the cluster phase acts as a dispersed filler phase only when the volume fraction of the clusters is below 0.2.

Second, the critical exponent n is considered. In this study, n for the clusters was found to be 3.1, and n for ion content to be 2.9. The critical exponent n depends, in principle, only on the spatial dimensions. However, this has been found not to be the case for elastic moduli in percolating systems.[39] A percolation study involving elasticity in an inorganic composite system composed of a hard inorganic filler (silver powder) and a soft continuous phase (air) showed that the critical exponent n was 3.8.[40] On the other hand, for a polymer composite system consisting of a hard organic filler (amorphous polyester, PETG) and a soft continuous phase (EPDM), n was found to be 1.8.[41] Since n in the P(SEB-*co*-SSNa) system is 3 ± 0.1, the value of the critical exponent here falls between the two systems mentioned above.

The study of percolation for the P(S-*co*-MANa) ionomer system shows that the critical volume fraction f_c and the critical exponent n for the volume fraction of cluster are 0.64 and 1.3, respectively.[16] These values are quite different from those for P(SEB-*co*-SSNa). This comparison indicates differences in the morphology of the clusters between P(S-*co*-MANa) and P(SEB-*co*-SSNa), as well as differences in the properties of the clusters as described in the section dealing with two morphological changes.

The present system differs from the P(S-*co*-MANa) system in one aspect, which might explain the high value of the exponent. Unlike P(S-*co*-MANa), in which every nonionic repeat unit is styrene, in P(SEB-*co*-SSNa), the nonionic repeat units can be ethylene, butylene, or styrene, while all the ionic groups are attached only to the phenyl rings. At high degrees of sulfonation, most of the nonionic segments consist of an ethylene−butylene copolymer. Thus, the restricted mobility region contains a disproportionally high styrene content, while the styrene in the matrix region is correspondingly depleted. This implies that the difference in the modulus between the cluster and the matrix regions is much higher here than in the P(S-*co*-MANa) case. Thus, the present system might resemble more closely that of a hard sphere in a soft matrix, for which the exponent has been found to be 3.8.[40]

4.4. Comparison of Mechanical Properties of the P(SEB-*co*-SSNa), P(S-*co*-SSNa), and P(S-*co*-MANa) Ionomers. It is interesting to compare the mechanical properties of the P(SEB-*co*-SSNa) system with those of the P(S-*co*-SSNa) and P(S-*co*-MANa) systems. One such comparison was given in Figure 6. Figure 5b shows plots of log E'_i of the ionomers against ion content in mequiv/cm^3. The reason for using this set of units for the present comparison is that for all three systems being compared, the ion content can be expressed in this set of units. The volume fractions of clusters were not obtained for the sulfonated polystyrene system because decomposition at elevated temperatures makes the determination of the areas under the loss tangent curves extremely difficult, as described in the Introduction. The plot of log E'_i for P(SEB-*co*-SSNa) coincides with that for P(S-*co*-SSNa) above 0.5 mequiv/cm^3. At low ion contents, the curves do not coincide because in that ion concentration range, the property of the host polymer predominates, and the value of modulus for nonionic system differs appreciably between P(S-*co*-SSNa) and P(SEB-*co*-SSNa). This coincidence of the plots for P(SEB-*co*-SSNa) and P(S-*co*-SSNa) indicates similarities in the properties of the clusters between P(SEB-*co*-SSNa) and P(S-*co*-SSNa). It should be recalled that both systems have the same type of ion pairs and the same position of ion pairs, i.e., adjacent to styrene units. Therefore, both ionomer systems should have similar stabilities of the multiplets and be subject to the same extent of steric hindrance to ag-

gregation of the ion pairs. This is probably the reason why similarities exist in the properties of the clusters between P(S-*co*-SSNa) and P(SEB-*co*-SSNa) in spite of the differences in the compositions of the polymers. On the other hand, the plots for P(S-*co*-MANa) are very similar to those for P(SEB-*co*-SSNa) only in a narrow range [0.5 < ion content (mequiv/cm^3) < 0.7].

5. Summary

Sodium sulfonated poly(styrene−ethylene−butylene) random ionomers, P(SEB-*co*-SSNa), were obtained by hydrogenation, sulfonation, and neutralization of styrene−butadiene copolymers. The dynamic mechanical properties of P(SEB-*co*-SSNa) were measured, and the most important results of a detailed analysis of the mechanical properties are summarized below.

Most of the P(SEB-*co*-SSNa) ionomers show two glass transitions as well as a well-developed ionic plateau region in the storage moduli between the two glass transitions. As the ion content increases, the T_g of the matrix phase does not increase as much as those of the ionomers based on styrene. This behavior is thought to be due to the flexibility of soft ethylene−butylene units in contrast to rigid styrene units. With increasing ion contents, the cluster T_g increases as much as that of ionomers based on polystyrene. However, beyond 8 mol % ion content, the cluster T_g does not change much.

The properties of P(SEB-*co*-SSNa) show two regions of morphological changes for the matrix and cluster phases. At low ion contents, the matrix is the only continuous phase. At intermediate ion contents (2−8 mol %), both the matrix and cluster phases are cocontinuous. At high ion contents, the cluster is the only continuous phase, and the matrix phase is dispersed. The discontinuities in trends for the matrix or cluster properties occur at 2−3 and 8−9 mol % (0.5 and 1.6 mequiv/cm^3).

The present ionomer system can be treated as a filler system as seen by the applicability of the Halpin−Tsai equation. Clusters can also be treated by percolation equations. The results of application show two features of P(SEB-*co*-SSNa). One is that the constants are very close to those for the site percolation in an fcc lattice as shown by the value (0.2) of the percolation threshold for the volume fraction of the clusters. The other is that the critical exponent for elastic modulus of the present system is found to be in the range for a hard filler in a soft continuous phase. These results reinforce the morphological model as well as filler approaches in P(SEB-*co*-SSNa).

Acknowledgment. We express our appreciation to Drs. J.-S. Kim and G. Tsagaropoulos for fruitful discussions. We would also like to thank Dr. Kim for active participation in the preparation and revision of the manuscript. M.N. appreciates Toyobo Co. Ltd. for giving him the opportunity to do research in Canada. This work was supported by the Natural Sciences and Engineering Research Council of Canada (NSERC).

Supporting Information Available: One table of density and glassy modulus, four figures of the dynamic mechanical properties of the P(SEB-*co*-SSNa) ionomers with the description of the figures and a discussion of the modification of the Halpin−Tsai equations (11 pages). Ordering information is given on any current masthead page.

References and Notes

(1) (a) Holliday, L., Ed. *Ionic Polymers*; Applied Science Publishers: London, 1975. (b) Eisenberg, A.; King, M. *Ion-Containing Polymers, Physical Properties and Structure*; Academic Press: New York, 1977. (c) Wilson, A. D.; Prosser, H. J., Eds. *Developments in Ionic Polymers*; Applied Science Publishers: New York, 1983. (d) Pineri, M.; Eisenberg, A., Eds. *Structure and Properties of Ionomers*: NATO ASI Series 198; D. Reidel Publishing Co.: Dordrecht, Holland, 1987.
(2) Eisenberg, A.; Yeager, H. L., Eds. *Perfluorinated Ionomer Membranes*; ACS Symposium Series 180; American Chemical Society: Washington, DC, 1982.
(3) Wilson, F. C.; Longworth, R.; Vaughan, D. J. *Polym. Prepr. (Am. Chem. Soc., Div. Polym. Chem.)* **1968**, *9*, 505.
(4) Marx, C. L.; Caulfield, D. F.; Cooper, S. L. *Macromolecules* **1973**, *6*, 344.
(5) MacKnight, W. J.; Taggart, W. P.; Stein, R. S. *J. Polym. Sci., Polym. Symp.* **1974**, *45*, 113.
(6) Eisenberg, A.; Navratil, M. *Macromolecules* **1974**, *7*, 90.
(7) Roche, E. J.; Stein, R. S.; Russell, T. P.; MacKnight, W. J. *J. Polym. Sci., Polym. Phys. Ed.* **1980**, *18*, 1497.
(8) Yarusso, D. J.; Cooper, S. L. *Macromolecules* **1983**, *16*, 1871.
(9) Eisenberg, A. *Macromolecules* **1970**, *3*, 147.
(10) Hird, B.; Eisenberg, A. *J. Polym. Sci., Part B: Polym. Phys.* **1990**, *28*, 1665.
(11) Hara, M.; Jar, P.; Sauer, J. A. *Polymer* **1991**, *32*, 1622.
(12) Weiss, R. A.; Fitzgerald, J. J.; Kim, D. *Macromolecules* **1991**, *24*, 1071.
(13) Ma, X.; Sauer, J. A.; Hara, M. *Macromolecules* **1995**, *28*, 3953.
(14) Eisenberg, A.; Hird, B.; Moore, R. B. *Macromolecules* **1990**, *23*, 4098.
(15) Eisenberg, A.; Navratil, M. *Macromolecules* **1973**, *6*, 604.
(16) Kim, J.-S.; Jackman, R. J.; Eisenberg, A. *Macromolecules* **1994**, *27*, 2789.
(17) Hird, B.; Eisenberg, A. *Macromolecules* **1992**, *25*, 6466.
(18) Kim, J.-S.; Yoshikawa, K.; Eisenberg, A. *Macromolecules* **1994**, *27*, 6347.
(19) (a) Canter, N. H. U. S. Patent 3,642,728, 1972. (b) O'Farrell, C. P.; Serniuk, G. E. U. S. Patent 3,836,511, 1974. (c) Makowski, H. S.; Lundberg, R. D.; Westerman, L.; Bock, J. In *Ions in Polymers*; Eisenberg, A., Ed.; Advances in Chemistry Series 187; American Chemical Society: Washington, DC, 1980; Chapter 2. (d) Siadat, B.; Lundberg, R. D.; Lenz, R. W. *Polym. Eng. Sci.* **1980**, *20*, 324.
(20) Molnár, A. Ph.D. Thesis, Department of Chemistry, McGill University, Montreal, Canada, 1992.
(21) Scott, R. L.; Carter, W. C.; Magat, M. L. *J. Am. Chem. Soc.* **1949**, *71*, 220.
(22) Thaler, W. A. *Macromolecules* **1983**, *16*, 623.
(23) Rahrig, D.; MacKnight, W. J.; Lenz, R. W. *Macromolecules* **1979**, *12*, 195.
(24) Guo, X.; Scott, P. J.; Rempel, G. L. *J. Mol. Catal.* **1992**, *72*, 193.
(25) Mohammadi, N. A.; Rempel, G. L. *J. Mol. Catal.* **1989**, *50*, 259.
(26) Fitzgerald, J. J.; Weiss, R. A. In *Coulombic Interactions in Macromolecular Systems*; Eisenberg, A., Bailey, F. E., Eds.; ACS Symposium Series 302; American Chemical Society: Washington, DC, 1986; Chapter 3.
(27) Storey, R. F.; George, S. E.; Nelson, M. E. *Macromolecules* **1991**, *24*, 2920.
(28) Weiss, R. A.; Sen, A.; Willis, C. L.; Pottick, L. A. *Polymer* **1991**, *32*, 1867.
(29) Lee, C. Y.-C.; Goldfarb, I. J. *Polym. Eng. Sci.* **1981**, *21*, 951.
(30) Gauthier, M.; Eisenberg, A. *Macromolecules* **1990**, *23*, 2066.
(31) Agarwal, P. K.; Makowski, H. S.; Lundberg, R. D. *Macromolecules* **1980**, *13*, 1679.
(32) Weast, R. C.; Lide, D. R.; Astle, M. J.; Beyer, W. H., Eds. *CRC Handbook of Chemistry and Physics*, 70th ed.; CRC Press: Boca Raton, FL, 1989.
(33) Kim, J.-S.; Wu, G.; Eisenberg, A. *Macromolecules* **1994**, *27*, 814.
(34) Otocka, E. P.; Kwei, T. K. *Macromolecules* **1968**, *1*, 401.
(35) Noshay, A.; Robeson, L. M. *J. Appl. Polym. Sci.* **1976**, *20*, 1885.
(36) Nielsen, L. E.; Landel, R. F. *Mechanical Properties of Polymers*; Marcel Dekker: New York, 1994.
(37) Halpin, J. C.; Kardos, J. L. *Polym. Eng. Sci.* **1976**, *6*, 344.
(38) Stauffer, D. *Introduction to Percolation Theory*; Taylor & Francis: London, 1985.
(39) Sahimi, M. *Applications of Percolation Theory*; Taylor & Francis: London, 1994.
(40) Deptuck, D.; Harrison, J. P.; Zawadzi, P. *Phys. Rev. Lett.* **1985**, *54*, 913.
(41) Hsu, W. Y.; Wu, S. *Polym. Eng. Sci.* **1993**, *33*, 293.

MA9513630